Comparison of Methods to Estimate Individual Tree Attributes Using Color Aerial Photographs and LiDAR Data

ANJIN CHANG, JUNG OK KIM, KIYUN RYU, YONG IL KIM
Department of Civil & Environmental Engineering
Seoul National University
Shillim-Dong, Gwanak-Ku, Seoul
KOREA
hal0208@snu.ac.kr, geostar1@snu.ac.kr, kiyun@snu.ac.kr, yik@snu.ac.kr

Abstract: - - The main objective of this study was to compare methods to estimate the number of trees and individual tree height using LiDAR data and aerial photography. A Korean pine tree study area for these techniques was selected the methods of watershed segmentation, region-growing segmentation, and morphological filtering were compared to estimate their accuracy. The algorithm was initiated by developing a normalized digital surface model (NDSM). A tree region was then extracted using classification and elimination errors of the NDSM and the photograph. The NDSM of the tree region was prefiltered and information about individual trees was extracted by segmentation and morphological methods. By using local maximum filtering, the tree height was obtained. Field observations were compared with the predicted values for accuracy assessment. The accuracy test showed the watershed segmentation algorithm to be the best estimator for tree modeling. Regression models for the study area explained 80% of the tree numbers and 89% of the heights.

Key-Words: - Aerial photography, LiDAR, Segmentation, Tree modeling

1 Introduction

For efficient and economical forest management, the accurate attributes of forests such as tree number, height, and diameter at breast height (DBH), have to be obtained easily. However, the traditional field-based process of obtaining a forest inventory is expensive, time-consuming, and inefficient [1]. In addition, field surveys for forest management have limitations in acquisition of information, because the area of concern is both huge and topographically difficult to access. In order to devise efficient methods of deriving forest information, recent tree-modeling studies have progressively considered remote sensing techniques. To acquire fundamental data on, for example, location, tree height, basal area, tree number, and frequency of occurrence.

Tree modeling by remote sensing has been studied by various researchers. For example, the intensity of a specific band of airborne multispectral MEIS-II images may be considered using a local maximum filter to find individual trees and to estimate basal area [2]. LiDAR sensors have the advantage over other methods of introducing the possibility of a fully three-dimensional analysis. Using an airborne laser system with a high sampling density, individual tree crowns can be detected [3], [4]. This makes it possible to detect their unique height and crown diameter. Using LiDAR data, the urban tree and tree free regions may be distinguished by elevation and intensity data [5], and the basal area may be estimated through making a correlation between crown diameter and DBH [1].

There are limitations in previous research, because of its use of single data sources such as satellite images, aerial photographs, or LiDAR data. Recent studies use both optical images and LiDAR data for tree modeling. Popescu et al. [6] show tree species classified by multispectral images and tree height estimated by a local maximum filter. Varying size and shape with elevation is obtained from LiDAR data and field observation on species. Individual trees can be detected by a segment-based classification method and tree height estimated using a local maximum filter [7].

The most important objective in tree modeling is to detect individual attributes. Usually segmentation methods, e.g., region-growing segmentation [1] and watershed segmentation [8], [9], are used whereas morphological filtering is typical [10]. The techniques differ in their approaches and reveal limitations in algorithm. In this respect, one of the

(a) Site 1 (b) Site 2 (c) Site 3 (d) Site 4

Fig. 1 Color Aerial Photograph

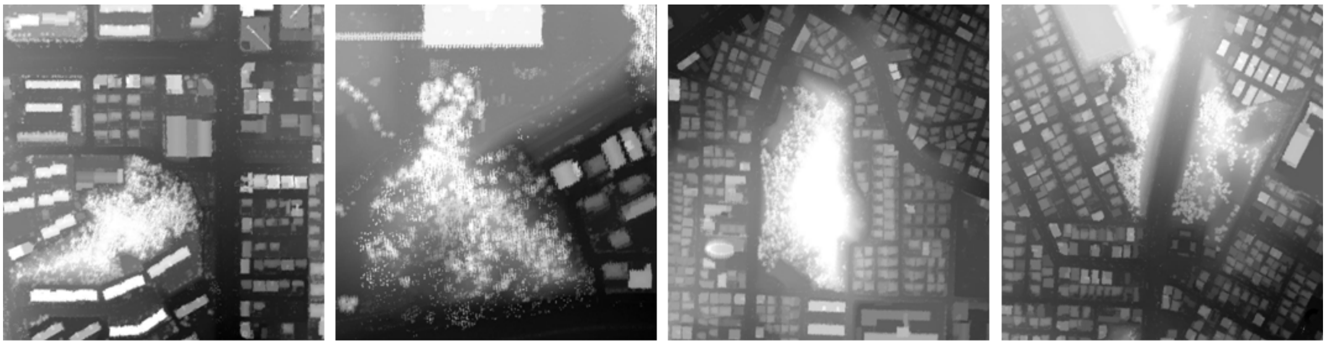

(a) Site 1 (b) Site 2 (c) Site 3 (d) Site 4

Fig. 2 LiDAR Data

major issues is that no one has determined the best method for tree modeling. This paper therefore reports on experiments carried out using color aerial photography and LiDAR data to decide on the best technique. An objective was to compare the detection techniques for individual tree attributes. Three approaches were considered: region-growing segmentation, watershed segmentation, and morphological filtering. Their accuracy in terms of tree numbers and heights was tested.

2 Study Site and Material

2.1 Aerial Photographs and LiDAR Data

The data used for this study were acquired from airborne systems. Four small area of coniferous forest in Daejeon City, Korea were selected for tree modeling. These are mostly composed of pitch pine, but include broad-leafed oak and tulip trees. Some of the area has been reforested. Aerial photographs (Fig. 1) and LiDAR data (Fig. 2) were acquired simultaneously on 26 April, 2005. The photograph resolution is 0.25×0.25 m and the point density of LiDAR Data is about 4 points/m^2.

2.2 Field Data

For accuracy analysis, we surveyed eight sample plots of field data at four sites. Each forest plot had homogenous species and was a fixed 10 × 10m square, apart from the third plot in Site 2, which was 20 × 20m. The tree number and height estimated in the study was compared with the field data. We only considered the needle-leaf trees because of season. The deciduous, broad-leaf trees did not have a developed leaf reflectance to the LiDAR signal, because it was early spring.

Table 1 Field Measurment Data

ID	Size	Tree Numbers	Mean of Tree Height (m)
1	10x 10 m	17	9.28
2	10x 10 m	13	11.58
3	20x 20 m	30	10.96
4	10x 10 m	12	7.20
5	10x 10 m	17	7.79
6	10x 10 m	22	11.47
7	10x 10 m	20	12.20
8	10x 10 m	29	9.78

3 Methodology

We proposed tree modeling by segmentation methods and compared each. Fig. 3 is a flowchart of the study, that can be divided into three parts: creation of a normalized digital surface model (NDSM), extraction of tree regions, and the detection of individual trees. The derived information was finally compared with the field data lastly. The processes are explained in detail below.

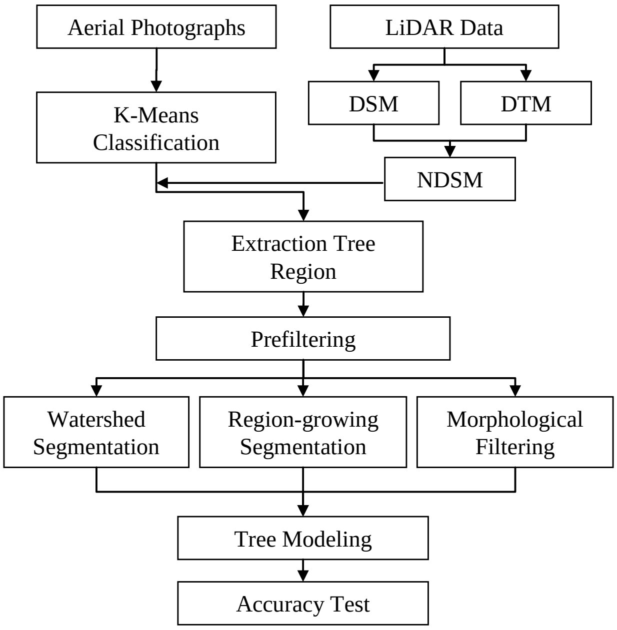

Fig. 3 Flow Chart

3.1 Creation of an NDSM

A terrain map is a necessity for tree modeling. We made a digital surface model (DSM) using the first-return LiDAR data. This is reflected from the surface of objects such as the soil, buildings, cars, leaves, and so on. The process aims to create a high resolution DSM interpolated from LiDAR data into a regular grid of 0.25 × 0.25m cells equated to the aerial photographs using an inverse distance weight interpolation algorithm [11].

The first return gives the elevation of surface, but not of the ground, because of superimposed objects. We created the digital terrain model (DTM) using morphological filtering from the DSM. Although the original morphological algorithm was developed for two-dimensional binary images, morphological filtering can be extended to three-dimensional grayscale images, where the grayscale values represent the intensity or another pixel attribute, such as elevation data. The effect of the morphological opening operation is to remove those image details that are smaller than the structuring element without distortion of a feature. The grayscale opening operation of the surface is derived from the highest point attained by a part of the structuring element as it slides underneath a surface [10]. We applied morphological opening filtering to the DSM to eliminate aboveground objects. The size of structuring element was empirically determined by iterative process since the structuring element had a circular boundary and we did not need to eliminate all the aboveground objects, such as building circular.

The creation of an NDSM was achieved by subtracting a gridded image created from the first-return DTM. Superficial buildings, trees, and cars, were barely recognizable in the NDSM.

3.2 Extraction of Tree Region

The aerial photograph is classified by a K-means

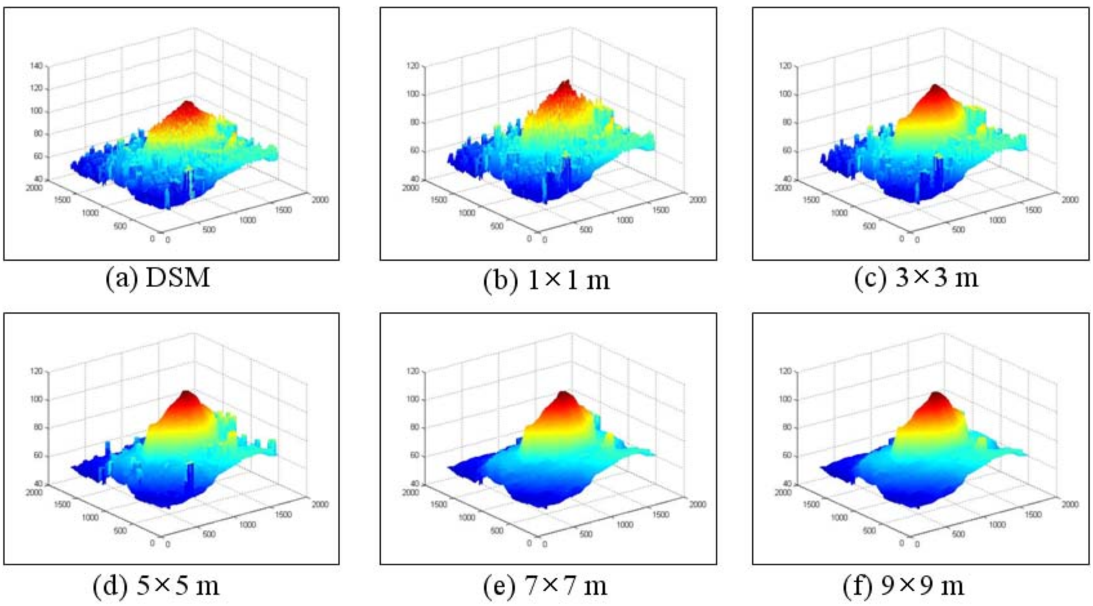

Fig. 4 Morphological filtering process by opening operation using variable mask sizes. Example obtained from site 3.

algorithm. We determined 15 empirically selected individual classes in the considered tree region. The results of the K-means classification include noise, since it is much simpler than other classification algorithms because the aerial photograph has only three bands (RGB). If the RGB color of an object surface is similar to that of the trees, the K-means algorithm classifies the object to the tree class. Therefore, we have to eliminate the noise of K-means classification with the NDSM.

The objects that have a similar character to trees cannot be easily eliminated by the simple threshold value. We used various factors such as area, variation of elevation, and shape to eliminate noise [8]. Using an area threshold, the small objects, shrubs, and the structures of similar elevation to trees were eliminated. Cars and planar objects have a different elevation variation of pixels that distinguish them. Tree pixel elevation value is notably variable and greater than other objects. The shadow and shape of building components can be eliminated by their eccentricity, since a tree is typically near circular. We finally derived a layer that has information about a tree region. Following this, it was necessary to devise a method to segment this data layer into individual tree canopies.

3.3 Detection Individual Trees

The efficiency of the core techniques in tree modeling is judged by their ability to detect individual trees. Typically, the segmentation and filtering methods of digital image processing are used in tree modeling. Segmentation subdivides an image into its constituent regions or objects on the discontinuity and similarity properties of pixels [12]. Morphological filtering can extract image components that are useful in the representation and description of regional shape.

The aim of both the segmentation and filtering process in our study was to delineate individual tree crowns. The NDSM derived from the LiDAR data was prefiltered using weighted averages to prevent failure of individual tree detection. All tree branches are united in the detection of an individual tree with a single maximum value without adjacent tree crowns merging [1]. As a result, we were able to detect individual trees with LiDAR data, using various techniques.

3.3.1 Region-growing Segmentation

Region-growing segmentation is a procedure that groups pixels or subregions into larger regions based on predefined criteria. This starts with a set of seed points, and from these, regions grow by appending to each seed those neighboring pixels that have properties similar to the seed points [12].

At first, the local maximum filter detects a point that has values greater than any of its eight neighborhood values. The pixels that have the local maximum value are the seed points [1]. The eight pixels around a seed point are compared with the seed point pixel. If the values are similar to the seed, the pixels can be placed in the same region. The areas of the same label correspond in this model to individual tree crowns. The region-growing segmentation used in our model has parameters that use controls according to the character of the images. The parameter values depend on the brightness, resolution, and texture quality of the image found by trial and error. This process was applied to the whole site.

3.3.2 Watershed Segmentation

In geographical terminology, a watershed is the ridge that divides areas drained by different river systems. The geographical area draining into a river or reservoir is called a catchment basin. If rain falls on a surface, it is clear that water would collect in such basins. Rain falling on the watershed ridgeline has equal probability of collecting in either of the two catchments. Watershed segmentation locates the catchment basins and ridgelines [13] and applies these ideas to the grayscale image.

The grayscale image is considered as a topological surface, where the pixel values are interpreted as heights. Methods for computing the watershed segmentation are the distance transform and the gradient magnitude. The gradient magnitude image has high pixel values along an object edge and low values everywhere else. We can detect individual trees and estimate tree height with local maximum filtering after watershed segmentation using the gradient magnitude.

3.3.3 Morphological Filtering

If a structuring element with a specified radius is used in morphological opening filtering of the NDSM, those areas of the NDSM in which the disk structuring element does not fit when pressed underneath the surface, such as the tops of individual conical or ellipsoidal tree crowns, will be removed through the opening operation. Top-hat filtering means subtracting the opened surface from the original surface. The tops of tree crowns remain in the NDSM, but the areas of other parts are removed. A thresholding operator is able to convert a top-hat filtered image into a binary one. Binary morphological opening filtering with a circular structuring element is sequentially applied to eliminate noise. These filtered operations can be carried out with a suitable structuring element to extract individual trees. Tree height is then estimated by local maximum filtering.

4 Result and Analysis

Variable information on tree number, tree height, location, and crown area is available through using our models. However, the accuracy in assessment of the number of trees and tree height had to be tested because field conditions in each test-plot were different and the pine trees were densely crowded. Furthermore, the plots measured 10 × 10 m, except for the third plot in Site 2, which was 20 × 20 m. The estimated forest information was compared with field data using statistical techniques.

4.1 The Number of Trees

Because of the variation in plot areas, estimated tree numbers were compared with field observation by calculating tree numbers per unit area. The results of the assessment for the number of trees are summarized in Table 2 for each model. When considering all the plots, the morphological filtering algorithm has the highest R^2 value, and watershed segmentation has the lowest. There is huge gap in the results achieved for watershed segmentation and morphological filtering. Watershed segmentation is distinctly a more suitable method than others are for tree modeling, even if the number of trees is overestimated and large crowns are split into several segments. The accuracy assessment for all the plots suggests that errors are present.

Each method has a characteristic error. The watershed algorithm overestimates the number of treetops whereas the region-growing and morphological algorithms are each sensitive to parameters. Additional error is caused when LiDAR data are converted into a grid by interpolation.

In the field, the forest trees are densely grouped. Not a few trees, which cannot be detected form the aerial system, are hidden around higher trees. Additionally, we only considered the needle-leaf trees in the study area, but the third plot in Site 2 includes those. The fourth and fifth plots in Site 3 had a recently changed tree distribution following artificial reforesting. We therefore rejected plots 3, 4, and 5 in the accuracy assessment.

After rejecting the plots with noise, R^2 greatly changed in the linear regression model. The R^2 of watershed segmentation increased markedly and the two other methods saw a reduced R^2. We can verify that the result for the watershed algorithm was the most accurate, but has instability. Morphological filtering has a stable algorithm, whereas the region-growing algorithm is neither accurate nor stable. The important point is that the field data closely correlated with the estimated values for the unchanged forest region.

Table 2 R^2 of the number of trees

Method	R^2	
	All plots	After rejecting 3, 4, 5 plots
Watershed Segmentation	0.2924	0.8003
Region-growing Segmentation	0.4295	0.0675
Morphological Filtering	0.7921	0.6725

4.2 Tree Height

The tree-height accuracy assessment was a dual comparison of the estimated mean and individual tree heights with field observations.

For group accuracy assessment, we discriminated between mean estimated tree height and mean observed value for a T-test in each plot. Table 3 shows the result. As already mentioned, we rejected plot 3, 4, and 5 for the T-test because of the low P-values. The result of the T-test for five plots concluded that the estimated tree height related to observed field data at a 5% significance level.

Table 3 T-test result of group tree height

ID	$P(T \leq \lvert t \rvert)$		
	Watershed Segmentation	Region-growing Segmentation	Morphological Filtering
1	0.8666	0.2286	0.5748
2	0.5245	0.3693	0.4985
3	0.0001	0.0314	0.0660
4	0.0085	0.0004	0.0009
5	0.0225	0.0003	0.0007
6	0.0697	0.1850	0.2180
7	0.5302	0.3025	0.4760
8	0.2119	0.5079	0.2905

We only considered the trees that could be definitely identified for individual tree-height accuracy testing, and the trees in Site 3 were considered because of reforesting. The same trees were chosen to compare the two data sets accurately and easily. A few trees were not seen in the image because of error in our model. Height error possibly occurred through interpolation of grid data from the LiDAR data following the signal not being reflected precisely from the treetops. A further possible reason could be the limited number of observations and the small size of plots.

Although some errors exist, the regression analysis of individual tree height gave a significant result overall for each algorithm. All of the methods revealed R^2 to be greater than 0.75. The regression did not show any bias in the data or relationship according to methods. A comparison between the predictions from LiDAR and field observation confirmed that our models are good estimators of individual tree height to ±0.5 m.

The validation between prediction and observation suggested that watershed segmentation can determine individual tree height more efficiently than can the other methods. Low R^2 results were obtained for region-growing segmentation and morphological filtering and for a few outliers. Morphological filtering was the most stable method used, but it is more sensitive, along with region-growing segmentation, than the watershed algorithm. Accordingly, we must select a method appropriate to the image character to achieve tree modeling.

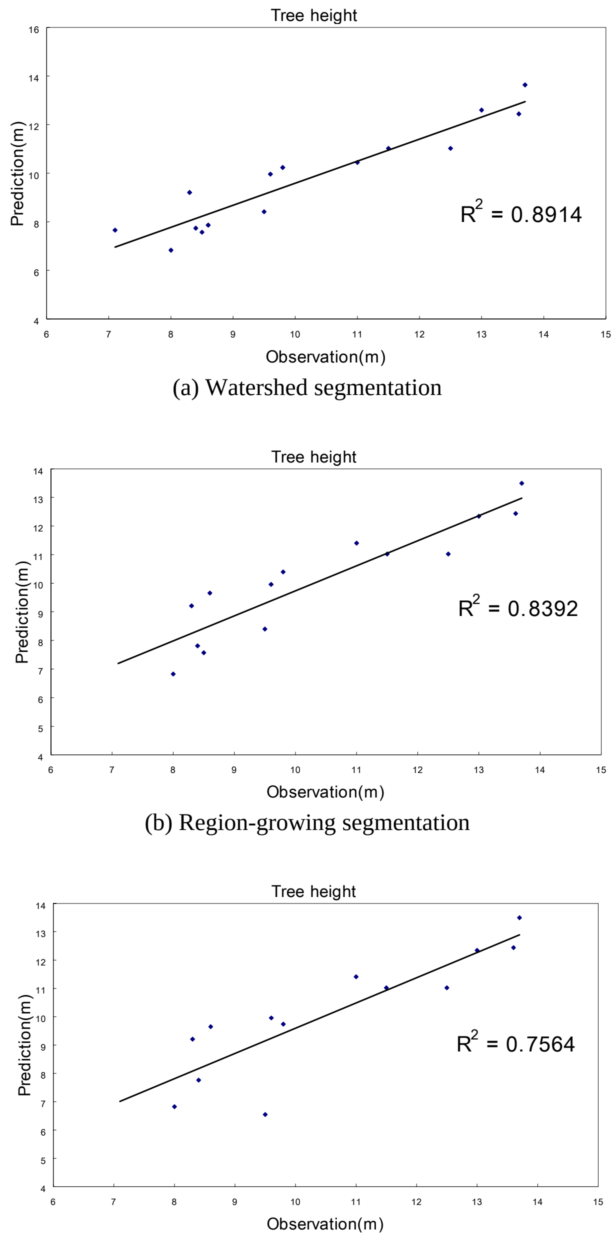

(a) Watershed segmentation

(b) Region-growing segmentation

(c) Morphological filtering

Fig. 5 Regression analysis of individual tree height

5 Conclusion

In this paper, we compared the three-methods of region-growing segmentation, watershed segmentation, and morphological filtering. We tested their accuracy in terms of numbers and heights. The NDSM was created by a morphological opening operation on LiDAR data and aerial photography that allowed tree region extraction. By using the segmentation and morphological methods with two-type data, the number and height of trees were calculated. Accuracy assessment showed watershed segmentation to be the best tree-modeling estimator whereas the region-growing algorithm gave the least less satisfactory result. Morphological filtering is a stable algorithm.

A limitation of this research we have to note is that segmentation and filtering methods used are very image dependent. To be more specific, the parameters were not defined automatically, but empirically following a trial and error process. Systematic error additionally comes from the aerial imaging system that, together with problems of incompleteness in field data, may degrade the research quality. Further study is thus needed to develop a new method that is robust to the types of images used and their corresponding parameters.

References:

[1] J. Hyyppä, O. Kelle, M. Lehikoinen, and M. Inkinen , "A segmentation-based method to retrieve stem volume estimates from 3-D tree height models produced by laser scanners," *IEEE Trans. Geoscience and Remote Sensing,* vol. 39, pp. 969-975, May. 2001.

[2] M. Wulder, K. O. Niemann, and D. G. Goodenough, "Local maximum filtering for the extraction of tree locations and basal area from high spatial resolution imagery," *Remote*

Sensing of Environment, vol. 73, pp. 103-114, 2000.

[3] A. Persson, J. Holmgren, and U. Soderman, "Detecting and measuring individual trees using an airborne laser scanner," *Photogrammetric Engineering and Remote Sensing*, vol. 68, no. 9, pp. 925-932, 2002.

[4] T. Brandtberg, T. A. Warner, R. E. Landenberger, and J. B. McGraw, "Detection and analysis of individual leaf-off tree crowns in small footprint, high sampling density LIDAR data from the eastern deciduous forests in North America," *Remote sensing of Environment*, vol. 85, pp. 290-303, 2003.

[5] U. Söderman, S. Ahlberg, M. Elmqvist, and A. Persson, "Three-dimensional environment models from airborne laser radar data," *in Proc. SPIE Defense Security Symposium Conf. Laser Radar Technology and Application* , Orlando, 2004, pp. 333-344.

[6] S. C. Popescu and R. H. Wynne, "Seeing the trees in the forest: using LiDAR and multispectral datat fusion with local filtering and variable window size for estimating tree height," *Photogrammetric Engineering and Remote Sensing*, vol. 70, no. 5, pp. 589-604, 2004

[7] J. C. Suárez, C. Ontiveros, S. Smith, and S. Snape, "Use of airborne LiDAR and aerial photography in the estimation of individual tree heights in forestry," *Computers and Geosciences*, vol. 31, pp. 253-262, 2005.

[8] A. J. Chang, "Estimation of individual tree and tree height using color aerial photograph and LiDAR data," *Korean Journal of Remote Sensing*, vol. 22, no. 6, pp.1-9, 2006.

[9] M. Schardt, M. Ziegler, A. Wimmer, R. Wack, and J. Hyyppä, "Assessment of forest parameters by means of laser scanning," *in Proc. ISPRS Technical Commission III Symposium 2002*, Graz, 2002, vol. A, pp. 302 ff.

[10] H. Andersen, S. E. Reutebuch, and G. F. Schreuder, "Automated individual tree measurement through morphological analysis of a LiDAR-based canopy surface model," *in Proc. First International Precision Forestry Cooperative Symposium*, Seattle, 2001, vol. 1, pp. 11-22.

[11] *Using ArcGIS 3D Analyst*, Redland: ESRI, NY, 2005, pp. 77-106.

[12] R. C. Gonzalez and R. E. Woods, *Digital Image Processing*, 2nd ed., Upper Saddle River, NJ: Prentice-Hall Inc., 2002, pp. 519-642.

[13] R. C. Gonzalez, R. E. Woods, and S. L. Eddins, *Digital Image Processing Using MATLAB*, Upper Saddle River, NJ: Pearson Education Inc., 2004, pp. 334-425.

[14] A. Bleau and L. J. Leon, "Watershed-based segmentation and region merging ," *Computer Vision and Image Understanding*, vol. 77, no. 3, pp. 317-370, 2000.

[15] D. A. Zimble, D. L. Evans, G. C. Carlson, R. C. Parker, S. C. Grado, and P. D. Gerard, "Characterizing vertical forest structure using small-footprint airborne LiDAR," *Remote Sensing of Environment*, vol. 87, pp. 171-182, 2003.

[16] G. Patenaude, R.A. Hill, R. Milne, D.L.A. Gaveau, B.B.J. Briggs, and T.P. Dawson, "Quantifying forest above ground carbon content using LiDAR remote sensing," *Remote Sensing of Environment*, vol. 93, pp. 368-380, 2004.

[17] M. Nilsson, "Estimation of tree heights and stand volume using an airborne LiDAR system," *Remote Sensing of Environment*, vol. 56, pp. 1-7, 1996.

[18] S. A. Hojjatoleslami and J. Kittler, "Region growing: a new approach," *IEEE Trans. Image Processing*, vol. 7, no. 7, pp. 1079-1084, 1998.